AD-A088 673 MICHIGAN STATE UNIV EAST LANSING DIV OF ENGINEERING --ETC F/G 17/9
RADAR WAVEFORM SYNTHESIS FOR TARGET IDENTIFICATION.(U)
MAY 80 K CHEN N00019-79-C-0385

UNCLASSIFIED NL

1 OF 1
AD
A088673

END
DATE
FILMED
10-80
DTIC

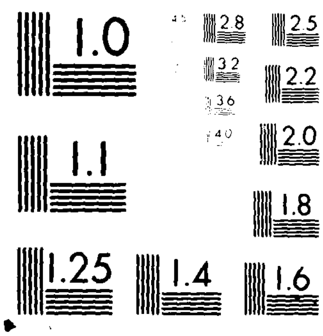

MICROCOPY RESOLUTION TEST CHART

Unclassified

SECURITY CLASSIFICATION OF THIS PAGE (When Data Entered)

REPORT DOCUMENTATION PAGE

READ INSTRUCTIONS BEFORE COMPLETING FORM

1. REPORT NUMBER
Final Report

2. GOVT ACCESSION NO.
AD-A088 673

3. RECIPIENT'S CATALOG NUMBER

4. TITLE (and Subtitle)
(6) Radar Waveform Synthesis for Target Identification.

5. TYPE OF REPORT & PERIOD COVERED
(9) Final Report. 5 Aug[redacted] [redacted]79-4 May [redacted]80

6. PERFORMING ORG. REPORT NUMBER

7. AUTHOR(s)
(10) Kun-Mu/Chen

8. CONTRACT OR GRANT NUMBER(s)
(15) N00019-79-C-0385

9. PERFORMING ORGANIZATION NAME AND ADDRESS
Division of Engineering Research
Michigan State University
East Lansing, Michigan 48824

10. PROGRAM ELEMENT, PROJECT, TASK AREA & WORK UNIT NUMBERS
(12) 51

11. CONTROLLING OFFICE NAME AND ADDRESS
Naval Air System Command
Department of the Navy

12. REPORT DATE
(11) 15 May [redacted]80

13. NUMBER OF PAGES
48

14. MONITORING AGENCY NAME & ADDRESS (if different from Controlling Office)

15. SECURITY CLASS. (of this report)
unclassified

15a. DECLASSIFICATION/DOWNGRADING SCHEDULE

16. DISTRIBUTION STATEMENT (of this Report)

Approved for public release; distribution unlimited.

17. DISTRIBUTION STATEMENT (of the abstract entered in Block 20, if different from Report)

NA

18. SUPPLEMENTARY NOTES

The findings of this report are not to be construed as an official Department of the Navy position, unless so designated by other authorized documents.

19. KEY WORDS (Continue on reverse side if necessary and identify by block number)

Radar signal waveform, natural resonance mode, thin wire, infinite cylinder, sphere, discrimination of radar targets, synthesis of waveform, incident radar signal, return radar signal

20. ABSTRACT (Continue on reverse side if necessary and identify by block number)

A new scheme for radar detection and discrimination, the radar waveform synthesis method, is investigated. This scheme consists of synthesizing the waveform of an incident radar signal which excites the target in such a way that the return radar signal from the target contains only a single natural resonance mode of the target. When the synthesized incident radar signal for a known, preselected target is applied to a wrong target, the return radar

DD FORM 1 JAN 73 1473

Unclassified 421

SECURITY CLASSIFICATION OF THIS PAGE (When Data Entered) signal will be significantly different from that of a natural mode of resonance, thus, the wrong target can be sensitively discriminated. The study on a simple geometry of a thin wire illuminated by a radar signal at normal incidence has been completed. The induced current on the target and the backscattered field from the target are obtained in terms of natural resonance modes. The required waveforms for the incident radar signal for exciting return radar signals which contain various single natural mode of resonance are obtained. When an incident radar signal, which is synthesized to excite a natural resonance mode of a thin wire, is applied to a slightly shorter or longer thin wire, the return radar signal from the wrong target is shown to be significantly different from that of a pure natural mode of resonance. Other studies on the cases of an infinite cylinder, a sphere, and a thin wire under an oblique excitation are in progress.

RADAR WAVEFORM SYNTHESIS FOR TARGET IDENTIFICATION

Abstract

A new scheme for radar detection and discrimination, the radar waveform synthesis method, is investigated. This scheme consists of synthesizing the waveform of an incident radar signal which excites the target in such a way that the return radar signal from the target contains only a single natural resonance mode of the target. When the synthesized incident radar signal for a known, preselected target is applied to a wrong target, the return radar signal will be significantly different from that of a natural mode of resonance, thus, the wrong target can be sensitively discriminated. The study on a simple geometry of a thin wire illuminated by a radar signal at normal incidence has been completed. The induced current on the target and the backscattered field from the target are obtained in terms of natural resonance modes. The required waveforms for the incident radar signal for exciting return radar signals which contain various single natural mode of resonance are obtained. When an incident radar signal, which is synthesized to excite a natural resonance mode of a thin wire, is applied to a slightly shorter or longer thin wire, the return radar signal from the wrong target is shown to be significantly different from that of a pure natural mode of resonance. Other studies on the cases of an infinite cylinder, a sphere, and a thin wire under an oblique excitation are in progress.

1. Introduction

Research on the target identification utilizing a short radar signal has been conducted in recent years by a number of workers [1-8]. Initially, the study on the scattering of a radar target has been determined either by time harmonic analysis coupled with Fourier inversion, or by direct time domain solution. After the Singularity Expansion Method (SEM) [9-12] was developed, the scattering behavior of a radar target became better understood. From numerous theoretical and experimental studies on the scattering of a transient wave from a metallic target, it is now commonly accepted that the scattered field from a radar target irradiated by a short radar signal can be expressed as a sum of natural modes of resonance of the target. The research based on this concept of natural resonance modes has since been intensified, however, all the work appears to be analysis. That is, to irradiate a target with a simple waveform, such as an impulse, a step function or a ramp function, and then analyze the scattered field in terms of natural modes of resonance or complex pole resonances. To discriminate between two targets, two sets of complex poles belonging to the two targets are compared.

In this research program, a new scheme for radar detection and discrimination, the radar waveform synthesis method, is investigated. Instead of analyzing the scattered field from the target in terms of natural resonance modes, this new scheme synthesizes the waveform of an incident radar signal in such a way that when it excites the target, the return radar signal from the target contains only a simple natural resonance mode of the target. Thus, when the synthesized incident radar signal for a known, preselected target is applied to a wrong target, the return radar signal will be significantly different from that of a natural resonance mode. Consequently, the wrong target can be sensitively discriminated.

To demonstrate the feasibility of this scheme, we have completed the study on the case of a thin wire illuminated by a radar signal at normal incidence. Other studies on the cases of an infinite cylinder, a sphere and a wire under an oblique excitation are in progress.

2. Accomplished Work

The results of the study on a thin wire with the normal incident excitation are described in this section.

As the first step, the induced current on the wire and the backscattered electric field from the wire are obtained in terms of natural resonance modes. The required waveforms for the incident radar signal for exciting return radar signals which contain various single natural mode of resonance are then determined. It is then demonstrated that when an incident radar signal, which is synthesized to excite a particular natural mode of the wire, is applied to a wrong target, a slightly shorter or longer wire, the return radar signal from the wrong target becomes significantly different from that of a pure damped sinusoid. Thus, the wrong target can be easily discriminated. Details of the study follow.

2.1 Induced Current on the Target

The geometry of the problem is shown in fig. 1, where a thin wire of length L and a radius a is illuminated by an incident radar signal at normal incidence. The electric field of the incident radar signal at the wire, in its Laplace transform, is assumed to be

$$\vec{E}^{inc}(z,s) = \hat{z}\, F(s) \tag{1}$$

where F(s) is the unknown function which describes the required waveform for the incident radar signal for exciting a return radar signal which contains only a single natural mode of resonance of the target. F(s) is independent of z because the incident electric field is in parallel with the wire.

The induced current on the wire, I(z,s), can be determined from the Pocklington's integral equation:

$$\int_0^L \left(\frac{\partial^2}{\partial z^2} - \frac{s^2}{c^2}\right) \frac{e^{-sR/c}}{4\pi R} \; I(z',s)dz' = -\epsilon_o s \; F(s) \quad (2)$$

where $\quad R = \sqrt{(z-z')^2+a^2}$

For convenience, we consider first the case of impulse excitation. That is, $F(s) = 1$ corresponding to $\vec{E}^{inc}(z,s) = \hat{z}\,\delta(t)$. For this case, eq. (2) is reduced to

$$\int_0^L \Gamma(z,z',s) \; I_1(z',s)dz' = -\epsilon_o s = V(s) \quad (3)$$

where $\quad \Gamma(z,z',s) = \left(\frac{\partial^2}{\partial z^2} - \frac{s^2}{c^2}\right) \frac{e^{-sR/c}}{4\pi R}$ = kernel of the integral

$V(s) = -\epsilon_o s$ = excitation

After the induced current $I_1(z,s)$ due to the impulse excitation is obtained, the induced current $I(z,s)$ due to an arbitrary excitation $F(s)$ will be simply equal to $I_1(z,s)\,F(s)$.

Based on physical intuition, the induced current $I_1(z',s)$ can be assumed to be the sum of all the natural resonance modes of the wire [9]:

$$I_1(z',s) = \sum_{\alpha=1}^{N} a_\alpha \nu_\alpha(z')(s-s_\alpha)^{-1} + W(z',s) \quad (4)$$

where a_α is the amplitude of the αth natural resonance mode, $\nu_\alpha(z')$ is the αth natural resonance mode, s_α is the αth natural resonance frequency, N is the maximum number of modes to be considered, and $W(z',s)$ is some function other than natural modes. The function $W(z',s)$ is usually assumed to be zero.

To solve eq. (3), let's consider the behavior of eq. (3) near $s = s_\alpha$. As s approaches to s_α, $I_1(z',s)$ is dominated by the αth natural mode, so that we can write

$$I_1(z',s) = a_\alpha \nu_\alpha(z')(s - s_\alpha)^{-1} + W'(z',s) \qquad (5)$$

where

$$W'(z',s) = \sum_{\substack{\beta=1 \\ \beta\neq\alpha}}^{N} a_\beta \nu_\beta(z')(s - s_\beta)^{-1} + W(z',s) \qquad (6)$$

$$= \text{analytic around } s = s_\alpha.$$

We can also expand the kernel of integral $\Gamma(z,z',s)$ and the excitation $V(s)$ in Taylar series around $s = s_\alpha$:

$$\Gamma(z,z',s) = \sum_{\ell=o}^{\infty} (s - s_\alpha)^\ell \Gamma_{\ell\alpha}(z,z') \qquad (7)$$

where

$$\Gamma_{\ell\alpha}(z,z') = \frac{1}{\ell!} \frac{\partial^\ell}{\partial s^\ell} \Gamma(z,z',s)\Big]_{s=s_\alpha} \qquad (8)$$

$$V(s) = -\varepsilon_o s = \sum_{\ell=o}^{\infty} (s - s_\alpha)^\ell V_{\ell\alpha} \qquad (9)$$

where

$$V_{\ell\alpha} = \frac{1}{\ell!} \frac{\partial^\ell}{\partial s^\ell} V(s)\Big]_{s=s_\alpha} \qquad (10)$$

It is noted that $\Gamma(z,z',s)$ and $V(s)$ can be expanded into Taylar series' because these two functions are analytic at $s = s_\alpha$.

Substituting eqs. (5), (7) and (9) in eq. (3) gives

$$\int_o^L \Big[\sum_{\ell=o}^{\infty} (s - s_\alpha)^\ell \Gamma_{\ell\alpha}(z,z')\Big]\big[a_\alpha \nu_\alpha(z')(s - s_\alpha)^{-1} + W'(z',s)\big]dz'$$

$$= \sum_{\ell=o}^{\infty} (s - s_\alpha)^\ell V_{\ell\alpha} \qquad (11)$$

Equating $(s - s_\alpha)^{-1}$ terms of eq. (11), we have

$$a_\alpha (s - s_\alpha)^{-1} \int_o^L \Gamma_{o\alpha}(z,z') \nu_\alpha(z') dz' = o$$

From eq. (8), $\Gamma_{o\alpha}(z,z') = [\Gamma(z,z',s)]_{s=s_\alpha} = \Gamma(z,z',s_\alpha)$.

Therefore, we have

$$\int_o^L \Gamma(z,z',s_\alpha)\nu_\alpha(z')dz' = o \qquad (12)$$

Equation (12) is the basic definition of the αth natural mode of the wire. It is also the special case of eq. (2), when $I(z',s) = \nu_\alpha(z')$ and zero excitation is needed to excite this current.

If $(s - s_\alpha)^o$ terms of eq. (11) are equated, we have

$$a_\alpha \int_o^L \Gamma_{1\alpha}(z,z')\nu_\alpha(z')dz' + \int_o^L \Gamma_{o\alpha}(z,z')W'(z',s)dz' = V_{o\alpha} \qquad (13)$$

If we multiply $\nu_\alpha(z)$ to eq. (13) and integrate it over z from o to L, we have

$$a_\alpha\int_o^L dz\nu_\alpha(z)\left[\int_o^L\Gamma_{1\alpha}(z,z')\nu_\alpha(z')dz'\right]+\int_o^L dz\nu_\alpha(z)\left[\int_o^L\Gamma_{o\alpha}(z,z')W'(z',s)dz'\right]$$

$$= \int_o^L dz\nu_\alpha(z)V_{o\alpha} \qquad (14)$$

The second term of the left-hand side of eq. (14) is zero, because

$$\int_o^L dz\nu_\alpha(z)\Gamma_{o\alpha}(z,z') = \int_o^L dz\nu_\alpha(z)\Gamma(z,z',s_\alpha) = o$$

based on eq. (12). Therefore, the amplitude of the αth natural mode a_α can be determined from eq. (14) as

$$a_\alpha = \frac{\int_o^L dz\nu_\alpha(z)V_{o\alpha}}{\int_o^L dz\nu_\alpha(z)\left[\int_o^L\Gamma_{1\alpha}(z,z')\nu_\alpha(z')dz'\right]} \qquad (15)$$

From eq. (10),

$$V_{o\alpha} = [V(s)]_{s=s_\alpha} = -\varepsilon_o s_\alpha$$

and from eq. (8),

$$\Gamma_{1\alpha}(z,z') = \frac{\partial}{\partial s}\left[\left(\frac{\partial^2}{\partial z^2} - \frac{s^2}{c^2}\right)\frac{e^{-sR/c}}{4\pi R}\right]_{s=s_\alpha}$$

For a thin wire, it is reasonable to assume the natural modes as

$$\nu_\alpha(z) = \sin\left(\frac{\alpha\pi z}{L}\right) \tag{16}$$

A real sinusoidal natural mode for $\nu_\alpha(z)$ as given in eq. (16) appears to be an approximate solution because another worker [10] found $\nu_\alpha(z)$ for a thin wire to contain a small imaginary component based on a numerical method. On the other hand, $\nu_\alpha(z)$ is a pure real function for a conducting sphere, therefore, the small imaginary component of $\nu_\alpha(z)$ may be the result of numerical error and eq. (16) may be nearly exact.

The numerator of eq. (15) can be easily obtained as

$$\int_o^L dz\,\nu_\alpha(z)V_{o\alpha} = \begin{cases} -\varepsilon_o s_\alpha \dfrac{2L}{\alpha\pi} & \text{for } \alpha = \text{odd} \\ o & \text{for } \alpha = \text{even} \end{cases} \tag{17}$$

The denominator of eq. (15) requires a tedious integration and it can be shown to be approximately equal to

$$\int_o^L dz\,\nu_\alpha(z)\left[\int_o^L \Gamma_{1\alpha}(z,z')\nu_\alpha(z')dz'\right] \doteq \frac{-s_\alpha L}{4\pi c^2}[2\log\left(\frac{L}{a}\right)-1] \tag{18}$$

We can then express a_α as

$$a_\alpha = K(\frac{1}{\alpha}) \quad \text{for } \alpha = \text{odd} \qquad (19)$$
$$= o \quad \text{for } \alpha = \text{even}$$

where $$K = \frac{8}{\mu_o[2 \log (\frac{L}{a}) - 1]} \qquad (20)$$

This result implies that only the odd modes (α = odd) of the current are excited on the wire by the impulse incident electric field.

The induced current on the wire due to the impulse excitation can now be expressed as

$$I_1(z,s) = K \sum_{\alpha=\text{odd}}^{N} \frac{1}{\alpha} \sin (\frac{\alpha \pi z}{L}) [\frac{1}{s-s_\alpha} + \frac{1}{s-s_\alpha{}^*}] \qquad (21)$$

where the conjugate term of $(s-s_\alpha)^{-1}$ was added because they should appear in pair to produce a real solution of $I_1(z,t)$.

The induced current on the wire due to the excitation of $\vec{E}^{inc}(z,s) = \hat{z}\, F(s)$ is simply given by

$$I(z,s) = K \sum_{\alpha=\text{odd}}^{N} F(s) \frac{1}{\alpha} \sin (\frac{\alpha \pi z}{L}) [\frac{1}{s-s_\alpha} + \frac{1}{s-s_\alpha{}^*}] \qquad (22)$$

Up to this point, the induced current on the wire is completely determined in a closed form. The excitation function F(s) is still an unknown function to be determined based on our requirement of exciting a single natural mode of backscattered field.

It is noted that the results obtained above correspond to the Class 1 coupling coefficient of Baum [9]. A somewhat different derivation can be applied to obtain an alternative solution for the amplitude of the αth natural mode a_α as a function of s, corresponding to the Class 2 coupling coefficient of Baum [9]. This alternative solution of a_α will lead to somewhat different solutions for the induced current and the backscattered field. Details of this alternative solution and the reasons for not using it in this study are given in Appendix B.

An equivalent circuit for the target can be constructed as shown in fig. 2 based on the expression of the induced current given in eq. (22). Equation (22) can be rearranged as

$$I(z,s) = [L\ F(s)] \sum_{\alpha=odd}^{N} \sin\left(\frac{\alpha\pi z}{L}\right) \left(\frac{K}{L}\right) \frac{1}{\alpha} \left[\frac{1}{s-s_\alpha} + \frac{1}{s-s_\alpha^*}\right] \tag{22a}$$

where [L F(s)] represents the applied voltage across the length of the wire maintained by the incident electric field.

The induced current can also be expressed as

$$I(z,s) = [L\ F(s)] \sum_{\alpha=odd}^{N} \sin\left(\frac{\alpha\pi z}{L}\right) Y_\alpha(s) \tag{23}$$

Equation (23) then implies a network of N parallel circuits with the admittance of each circuit represented by $Y_\alpha(s)$. Comparing eqs. (23) and (22a), we have

$$Y_\alpha(s) = \left(\frac{K}{L}\right)\left(\frac{1}{\alpha}\right)\left[\frac{1}{s-s_\alpha} + \frac{1}{s-s_\alpha^*}\right] = \left(\frac{K}{L}\right)\left(\frac{1}{\alpha}\right)\left[\frac{2s + 2\sigma_\alpha}{s^2+2\sigma_\alpha s+(\sigma_\alpha^2+\omega_\alpha^2)}\right] \tag{24}$$

where $s_\alpha = -\sigma_\alpha + j\omega_\alpha$.

$Y_\alpha(s)$ can be synthesized with a capacitor C_α, an inductor L_α, a series resistor R_α, and a resistor r_α connected across C_α as shown in fig. 2. The values of these equivalent circuit elements are

$$C_\alpha = \left(\frac{K}{L}\right)\frac{2}{\alpha}\frac{1}{\omega_\alpha^2},\quad L_\alpha = \left(\frac{L}{K}\right)\frac{\alpha}{2},\quad R_\alpha = \left(\frac{L}{K}\right)\frac{\alpha}{2}\sigma_\alpha \quad \text{and} \quad r_\alpha = \left(\frac{L}{K}\right)\frac{\alpha}{2}\frac{\omega_\alpha^2}{\sigma_\alpha}$$

where $\frac{L}{K} = \frac{1}{8}\left[2 \log\left(\frac{L}{a}\right)-1\right] L\ \mu_o$ (henry).

Now in terms of the induced current, the target can be considered as a network of N resonant circuits, each representing a natural mode of resonance, connected in parallel. The incident radar signal excites in each resonant circuit a current which has a spatial variation of $\sin\left(\frac{\alpha\pi z}{L}\right)$ and a temporal variation of $F(s)\left[\frac{1}{s-s_\alpha} + \frac{1}{s-s_\alpha^*}\right]$. As an example, the spatial and temporal variations of inducee currents in this equivalent network for the case of impulse excitation, $F(s) = 1$, are depicted in fig. 3. It is noted that for other excitations, only the temporal variation of the induced current in each resonant circuit changes while its spatial variation remains the same.

It is evident to observe from eq. (22) that it is not possible to excite only a single natural mode of induced current on the target with the radar signal of eq. (1) which is independent of z at the target. However, it is possible to excite a single natural mode of backscattered electric field in the return radar signal with an appropriate choice of F(s) as shown in a later section.

2.2 Backscattered Field from the Target

After the induced current on the target is obtained, it is easy to determine the scattered field from the target. For simplicity, only the backscattered electric field maintained by the induced current on the target will be considered here.

In the present case, the incident radar signal is incident upon the wire normally, so that the backscattered field in the far zone of the target is simply given by

$$\vec{E}^s(t) = -\frac{\partial}{\partial t}\vec{A}(t) = \hat{z}\left(-\frac{\partial}{\partial t}A(t)\right),$$

or in its Laplace transform,

$$\vec{E}^s(s) = \hat{z}\,E^s(s) = \hat{z}(-sA(s)) \tag{25}$$

where $\vec{A}(t)$ is the vector potential maintained by the induced current on the target. Since $\vec{A}(t)$ at the radar receiving antenna located at a distance R_∞ from the wire can be obtained as

$$A(t) = \frac{\mu_o}{4\pi} \int_o^L \frac{I(z',t-R_\infty/c)}{R_\infty} dz' ,$$

its Laplace transform can be found to be

$$A(s) = \frac{\mu_o}{4\pi} \frac{e^{-sR_\infty/c}}{R_\infty} \int_o^L I(z',s)dz' \tag{26}$$

Therefore, the backscattered electric field is

$$E^s(s) = - \frac{\mu_o}{4\pi} \frac{e^{-sR_\infty/c}}{R_\infty} \left[s \int_o^L I(z',s)dz' \right] \tag{27}$$

Substituting $I(z',s)$ of eq. (22) in eq. (27) yields

$$E^s(s) = K_1 \frac{e^{-sR_\infty/c}}{R_\infty} \sum_{\alpha=odd}^{N} s\ F(s) \frac{1}{\alpha^2} \left[\frac{1}{s-s_\alpha} + \frac{1}{s-s_\alpha{}^*}\right] \tag{28}$$

where $K_1 = (- \frac{\mu_o}{4\pi})(\frac{2L}{\pi})K = \frac{-4L}{\pi^2[2 \log (\frac{L}{a})-1]}$

To investigate the nature of $E^s(s)$, and avoiding the difficulty of $R_\infty \to \infty$, let's consider the quantity of

$$R_\infty E^s(s) = K_1\ e^{-sR_\infty/c}\ E_1^s(s) \tag{29}$$

where $$E_1^s(s) = \sum_{\alpha=odd}^{N} s\ F(s) \frac{1}{\alpha^2} \left[\frac{1}{s-s_\alpha} + \frac{1}{s-s_\alpha{}^*}\right] \tag{30}$$

The relationship between $E^s(t)$ and $E_1^s(t)$ is evident based on Shifting theorm:

$$R_\infty E^s(t) = K_1\ E_1^s(t - R_\infty/c)u(t - R_\infty/c) \tag{31}$$

This implies that there is a retarded time of R_∞/c between $E^s(t)$ and $E_1^s(t)$. Thus, if we desire to synthesize $E^s(s)$, it is only necessary to synthesize $E_1^s(s)$. At this point, we are in a position to choose appropriate F(s)'s to produce desired backscattered fields of $E_1^s(s)$ or $E^s(s)$.

2.3 Required Waveform for Exciting Single Natural Mode

If we desire to have the backscattered electric field containing only a single natural mode of resonance (the jth mode), $E_1^s(s)$ should have the following forms:

To have a single natural mode with a maximum initial value,

$$E_1^s(s) = \frac{1}{s-s_j} + \frac{1}{s-s_j{}^*} \quad , \tag{32}$$

corresponding to

$$E_1^s(t) = 2\,e^{-\sigma_j t}\cos\omega_j t \cdot \text{ (where } s_j = -\sigma_j + j\omega_j)$$

To have a single natural mode with a zero initial value,

$$E_1^s(s) = \frac{-j}{s-s_j} + \frac{j}{s-s_j{}^*} \, , \tag{33}$$

corresponding to

$$E_1^s(t) = 2\,e^{-\sigma_j t}\sin\omega_j t.$$

The required waveform, $F_j(s)$, for the incident radar signal for exciting a backscattered electric field which contains only the jth natural mode of resonance can then be determined by equating eq. (30) to eq. (32) or to eq. (33):

$$E_1^s(s) = \sum_{\alpha=odd}^{N} s\, F_j(s)\, \frac{1}{\alpha^2}\left[\frac{1}{s-s_\alpha} + \frac{1}{s-s_\alpha{}^*}\right] = \frac{1}{s-s_j} + \frac{1}{s-s_j{}^*} \quad (34)$$

$$\text{or} \quad = \frac{-j}{s-s_j} + \frac{j}{s-s_j{}^*} \quad (35)$$

From eq. (34), we have

$$F_j(s) = \frac{\dfrac{1}{s-s_j} + \dfrac{1}{s-s_j{}^*}}{\displaystyle\sum_{\alpha=odd}^{N} s\, \frac{1}{\alpha^2}\left[\frac{1}{s-s_\alpha} + \frac{1}{s-s_\alpha{}^*}\right]}$$

$$= \frac{(s-s_1^r)\displaystyle\prod_{\substack{\alpha=odd\\ \alpha\neq j}}^{N}(s-s_\alpha)(s-s_\alpha{}^*)}{s\left\{\begin{array}{l}(s-s_1^r)\displaystyle\prod_{\substack{\alpha=odd\\ \alpha\neq 1}}^{N}(s-s_\alpha)(s-s_\alpha{}^*) + \frac{1}{9}(s-s_3^r)\prod_{\substack{\alpha=odd\\ \alpha\neq 3}}^{N}(s-s_\alpha)(s-s_\alpha{}^*)\\ + \dfrac{1}{25}(s-s_5^r)\displaystyle\prod_{\substack{\alpha=odd\\ \alpha\neq 5}}^{N}(s-s_\alpha)(s-s_\alpha{}^*) + \ldots + \frac{1}{N^2}(s-s_N^r)\prod_{\substack{\alpha=odd\\ \alpha\neq N}}^{N}(s-s_\alpha)(s-s_\alpha{}^*)\end{array}\right\}} \quad (36)$$

where $s_\alpha^r = \mathrm{Re}[s_\alpha]$

From eq. (35), we have

$$F_j(s) = \frac{\frac{-j}{s-s_j} + \frac{j}{s-s_j^*}}{\sum_{\alpha=odd}^{N} s \frac{1}{\alpha^2} \left[\frac{1}{s-s_\alpha} + \frac{1}{s-s_\alpha^*}\right]}$$

$$= \frac{s_j^i \prod_{\substack{\alpha=odd \\ \alpha\neq j}}^{N} (s-s_\alpha)(s-s_\alpha^*)}{s\left\{\begin{array}{l}(s-s_1^r) \prod_{\substack{\alpha=odd \\ \alpha\neq 1}}^{N} (s-s_\alpha)(s-s_\alpha^*) + \frac{1}{9}(s-s_3^r) \prod_{\substack{\alpha=odd \\ \alpha\neq 3}}^{N} (s-s_\alpha)(s-s_\alpha^*) \\ + \frac{1}{25}(s-s_5^r) \prod_{\substack{\alpha=odd \\ \alpha\neq 5}}^{N} (s-s_\alpha)(s-s_\alpha^*) + \ldots + \frac{1}{N^2}(s-s_N^r) \prod_{\substack{\alpha=odd \\ \alpha\neq N}}^{N} (s-s_\alpha)(s-s_\alpha^*)\end{array}\right\}} \quad (37)$$

where $s_j^i = \text{Im}[s_j]$.

The expression of $F_j(s)$ in eqs. (36) or (37) is a ratio of two polynomials of s. This expression can be directly inverted back to the real-time function $F_j(t)$ using a method based on the state-space approach and a digital computer. This method developed by Liou [13] will be briefly outlined in the Appendix A.

At this point, a question arises: with all the modes of induced current excited, why the backscattered field contains only the jth natural mode? The answer can be found after a careful examination of eqs. (22), (28), (36) and (37) and with a help of the equivalent circuit: in the jth mode resonant circuit, two components of induced current are excited. One component is a pure natural mode which has natural spatial and temporal variations; the other component has the natural spatial variation but a forced temporal variation (forced by $F_j(s)$). In all other resonant circuits, the induced current has a natural spatial variation but a forced temporal variation. When the effects of N modes of induced currents with natural spatial variations but forced temporal variations are added up, they maintain a zero backscattered electric field. Therefore, only the component of induced current in the jth mode resonant circuit which has both natural spatial and temporal variations will maintain a pure jth natural mode of the backscattered field. This type of cancellation is possible only if the incident radar signal has a temporal variation described by $F_j(s)$.

Some numerical examples are given here. We will consider a thin wire with the dimension of L/a = 100, and consider only the first ten natural resonance modes in the wire. Because the radar signal is incident normally to the wire only the odd natural resonance modes (α = odd) are excited. The natural frequencies of these excited modes are:

$$S_1 = (-.0828 + j.9251)\ (\frac{\pi c}{L})$$

$$S_3 = (-.1491 + j2.8835)\ (\frac{\pi c}{L})$$

$$S_5 = (-.1909 + j4.8536)\ (\frac{\pi c}{L})$$

$$S_7 = (-.2240 + j6.8286)\ (\frac{\pi c}{L})$$

$$S_9 = (-.2552 + j8.8068)\ (\frac{\pi c}{L})$$

With these values of S_α substituted in eqs. (36) or (37), $F_j(s)$ can be expressed explicitly as a ratio of two polynomials of S. We have developed a computer program to directly invert $F_j(s)$ into the real-time function of $F_j(t)$. Four numerical examples are given in figs. 4 to 7.

Figure 4 shows the required waveform of the incident radar signal for exciting a return radar signal which contains only the first natural resonance mode (with a maximum initial value) of the wire, and the waveform of the return radar signal which indeed exhibits the first natural resonance mode with a maximum initial value. It is noticed that the relative amplitude of the required waveform for the incident radar signal $F_1(t)$ is plotted as a function of the normalized time t $(\frac{\pi c}{L})$, and the relative amplitude of the waveform of the return radar signal $E_1(t)$ is plotted as a function of the normalized retarded time $(t - \frac{2R_\infty}{L})(\frac{\pi c}{L})$. The waveform of $F_1(t)$ is somewhat like a step function modulated with a damped oscillating function, while the return radar signal is a pure damped sinusoidal function with a maximum initial value.

Figure 5 shows the required waveform $F_3(t)$ of the incident radar signal for exciting a return radar signal which contains only the third natural resonance mode (with a maximum initial value) of the wire, and the waveform $E_3(t)$ of the return radar signal. The waveforms of $F_3(t)$ and $E_3(t)$ are similar, but with some difference in the periodicity and the steady state value.

Figure 6 shows the required waveform $F_1(t)$ of the incident radar signal for exciting a return radar signal which contains only the first natural resonance mode (with a zero initial value) of the wire, and the waveform $E_1(t)$ of the return radar signal which indeed exhibits the first natural resonance mode with a zero initial value. It is observed that the required waveform $F_1(t)$ resembles a ramp function for small t but it reaches a steady-state value exponentially at large t. The whole waveform of $F_1(t)$ resembles that of the charging voltage across a capacitor. The return radar signal $E_1(t)$ is a pure damped sinusoidal function with a zero initial value. This is an interesting finding because a number of workers [1,2,4] have observed the phenomenon that with a ramp radar pulse, the return radar signal from a target usually exhibits a damped sinusoidal waveform. Our finding provides a theoretical support for this phenomenon.

Figure 7 shows the required waveform $F_3(t)$ of the incident radar signal for exciting a return radar signal which contains only the third natural resonance mode (with a zero initial value), and the waveform $E_3(t)$ of the return radar signal which exhibits the third natural resonance mode with a zero initial value. It is interesting to observe that the waveform $F_3(t)$ looks like a damped sinusoidal function superimposed on the waveform $F_1(t)$ of fig. 6. The waveform $E_3(t)$ is a pure damped sinusoidal function with a zero initial value. It is noted that there is a slight difference between the periodicities of $F_3(t)$ and $E_3(t)$ in fig. 7.

2.4 Discrimination of Wrong Targets

When an incident radar signal with a synthesized waveform for exciting a natural resonance mode of a preselected target, which resonant frequencies are assumed to be known, is applied to a different target, the return radar signal is expected to be significantly different from that of a pure natural resonance mode, a damped sinusoidal function. Three examples are given here to demonstrate this phenomenon.

In the first example, the incident radar signal is synthesized to have a waveform $F_1(s)$ which will produce the first natural mode (with a maximum initial value) in the return radar signal from a thin wire of length L and radius a. $F_1(s)$ is given by eq. (36) when j is set to be 1 in its numerator, and $F_1(t)$ is depicted in fig. 4. Assuming that this incident radar signal with the waveform of $F_1(s)$ is applied to a wrong target, a slightly shorter wire with length L' and radius a' where

$$\frac{L}{L'} = \frac{a}{a'} = m = 1.05 \quad .$$

Natural resonant frequencies s'_α of the wrong target are given by

$$s'_\alpha = m\ s_\alpha \quad .$$

The return radar signal from the wrong target will be

$$E_1(s) \sim s\ F_1(s) \sum_{\alpha=\text{odd}}^{N} \frac{1}{\alpha^2} \left[\frac{1}{s-s'_\alpha} + \frac{1}{s-s'^{*}_\alpha}\right] = \frac{N_1(s)}{D_1(s)} \qquad (38)$$

where

$$N_1(s)=(s-s_1^r)\prod_{\substack{\alpha=odd\\ \alpha\neq 1}}^{N}(s-s_\alpha)(s-s_\alpha{}^*)\left[\begin{array}{l}(s-ms_1^r)\prod\limits_{\substack{\alpha=odd\\ \alpha\neq 1}}^{N}(s-ms_\alpha)(s-ms_\alpha{}^*)\\ +\frac{1}{9}(s-ms_3^r)\prod\limits_{\substack{\alpha=odd\\ \alpha\neq 3}}^{N}(s-ms_\alpha)(s-ms_\alpha{}^*)\\ +\ \cdots\cdots\cdots\cdots\cdots\cdots\\ +\frac{1}{N^2}(s-ms_N^r)\prod\limits_{\substack{\alpha=odd\\ \alpha\neq N}}^{N}(s-ms_\alpha)(s-ms_\alpha{}^*)\end{array}\right] \tag{39}$$

$$D_1(s)=\prod_{\alpha=odd}^{N}(s-ms_\alpha)(s-ms_\alpha{}^*)\left[\begin{array}{l}(s-s_1^r)\prod\limits_{\substack{\alpha=odd\\ \alpha\neq 1}}^{N}(s-s_\alpha)(s-s_\alpha{}^*)\\ +\frac{1}{9}(s-s_3^r)\prod\limits_{\substack{\alpha=odd\\ \alpha\neq 3}}^{N}(s-s_\alpha)(s-s_\alpha{}^*)\\ +\cdots\cdots\cdots\cdots\cdots\cdots\\ +\frac{1}{N^2}(s-s_N^r)\prod\limits_{\substack{\alpha=odd\\ \alpha\neq N}}^{N}(s-s_\alpha)(s-s_\alpha{}^*)\end{array}\right] \tag{40}$$

The real-time function of the return radar signal from the wrong target can be obtained by inverting eq. (38) with our computer program. The result is shown in fig. 8 in comparison with the return radar signal from the right target, which is a pure damped sinusoidal function. It is noted that when the synthesized incident radar signal is applied to the right target, its return signal will be

$$E_1(s) \sim \frac{(s-s_1^r)}{(s-s_1)(s-s_1^*)} = \begin{array}{l}\text{pure damped sinusoidal function} \\ \text{with a maximum initial value.}\end{array}$$

It is observed in fig. 8 that the return radar signal from the wrong target is significantly different from a pure damped sinusoidal function; different waveforms around the peaks and a changed periodicity. It is evident that if the dimensions of the wrong target are different from that of the right target by a greater margin than this example, the difference in the waveforms of the return radar signals from the right and the wrong target will be more outstanding.

The second example as depicted in fig. 9 shows the waveforms of return radar signals from the right and the wrong target when they are illuminated by an incident radar signal with a synthesized waveform of $F_3(s)$ which will produce the third natural resonance mode (with a maximum initial value) in the return radar signal from the right target. The waveform $F_3(s)$ of the incident radar signal is given by eq. (36) when j is set to be 3 in its numerator, and $F_3(t)$ is depicted in fig. 5. The return radar signal from the wrong target can be expressed as

$$E_3(s) \sim \frac{N_3(s)}{D_3(s)} \tag{41}$$

where

$$N_3(s) = N_1(s) \frac{(s-s_3^r)(s-s_1)(s-s_1^*)}{(s-s_1^r)(s-s_3)(s-s_3^*)} \tag{42}$$

$$D_3(s) = D_1(s) \tag{43}$$

The return radar signal from the right target is

$$E_3(s) \sim \frac{(s-s_3^r)}{(s-s_3)(s-s_3^*)} = \begin{array}{l}\text{pure damped sinusoidal function} \\ \text{with a maximum initial value.}\end{array}$$

As observed in fig. 9, the return radar signal from the wrong target damps faster than that from the right target, and in the late-time stage, the phase of the former becomes opposite to that of the latter. The difference between the waveforms of these two return radar signals is quite significant and can be easily identified.

The third example considers the waveforms of return radar signals from the right target and two wrong targets, one is about 5% longer and the other about 5% shorter than the right target, when they are illuminated by an incident radar signal with a synthesized waveform of $F_1(s)$ which will produce the first natural resonance mode (with a zero initial value) in the return radar signal from the right target. The waveform $F_1(s)$ of the incident radar signal is given by eq. (37) when j is set to be 1 in its numerator, and $F_1(t)$ is depicted in fig. 6. The waveforms of return radar signals from these three targets are shown in fig. 10. It is observed that the periodicities of the return radar signals from the wrong targets have been significantly altered from that of the right target. This should lead to an easy discrimination of wrong targets.

It is noted that in the calculation of the waveform for the longer target, its natural resonant frequencies s_α' have been assumed to be $s_\alpha' = 0.95\ s_\alpha$ where s_α represents the natural resonant frequencies of the right target. For the shorter target, the identical natural resonant frequencies as used in the first example have been adapted.

3. Work in Progress

Studies on an infinite cylinder, a sphere and a wire under oblique excitation are being conducted, and some preliminary results are outlined in this section.

3.1 An Infinite Cylinder

The case of a perfectly conducting, infinite cylinder with a radius a illuminated by a radar signal of TM polarization as shown in fig. 11 is studied.

The incident electric field is assumed to be

$$\vec{E}^{inc}(\vec{r},t) = \hat{y}\ F\ [t-(x+a)/c]U(t-(x+a)/c)$$
$$= (\hat{r}\sin\phi + \hat{\phi}\cos\phi)\ F\ (t-\frac{a}{c}-\frac{r}{c}\cos\phi)$$
$$\cdot U(t-\frac{a}{c}-\frac{r}{c}\cos\phi)$$

and in its Laplace transform

$$\vec{E}^{inc}(\vec{r},s) = (\hat{r}\sin\phi + \hat{\phi}\cos\phi)\quad F(s)e^{-\frac{sa}{c}}\ e^{-\frac{sr}{c}\cos\phi} \tag{44}$$

where F(s) represents the time function which describes the waveform of the incident radar signal.

Using the differential equation and the separation of variable approach, the induced current on the cylinder surface, K_ϕ, and the scattered electric field in the far zone, E_ϕ^{sr}, can be obtained as

$$K_\phi(\phi,s) = -F(s)\ \frac{c}{\zeta_o a}\ \frac{e^{-sa/c}}{s}\ \sum_{n=0}^{\infty} \frac{(-1)^n \varepsilon_n}{K_n'(sa/c)}\cos n\phi \tag{45}$$

and

$$E_\phi^{sr}\ (r,\phi,s) = -F(s)\ \sqrt{\frac{\pi c}{2sr}}\ e^{-s(r+a)/c}$$

$$\sum_{n=0}^{\infty} \frac{(-1)^n \varepsilon_n I_n'(sa/c)}{K_n'(sa/c)}\cos n\phi \tag{46}$$

where $K_n(sa/c)$ and $I_n(sa/c)$ are modified Bessel functions and the prime sign represents the derivative of the function.

The induced current K_ϕ can also be obtained from the following integral equation:

$$\int_{-\pi}^{\pi} K_\phi(\phi',s)\ \Gamma(\phi,\phi',s)d\phi' = -\varepsilon_o asF(s)e^{-\frac{sa}{c}}\ e^{-\frac{sa}{c}\cos\phi} \cos\phi \tag{47}$$

where

$$\Gamma(\phi,\phi',s) = \frac{1}{2\pi}\left[\frac{\partial^2}{\partial\phi 2} - \frac{s^2a^2}{c^2}\cos(\phi-\phi')\right]$$

$$K_o\left(\frac{sa}{c}\sqrt{2[1-\cos(\phi-\phi')]}\right)$$

$$= \frac{1}{2\pi}\sum_{n=0}^{\infty}\frac{s^2a^2}{c^2}\varepsilon_n I_n'\left(\frac{sa}{c}\right)\ K_n'\left(\frac{sa}{c}\right)\ \cos n(\phi-\phi') \tag{48}$$

To analyze the transient behavior of the target, the induced current and the scattered electric field are expressed in terms of natural modes as follow.

$$K_\phi(\phi,s) = \sum_{n=0}^{\infty}\ \sum_{m=0}^{\infty} A_{nm}(s)\ \cos n\phi\ (s-s_{nm})^{-1} \tag{49}$$

where $A_{nm}(s)$ is the amplitude or the coupling coefficient of the nmth natural mode, $\cos n\phi$ is the nth natural mode, and s_{nm} is the nmth natural frequency of the resonance. We can show that

$$A_{nm}(s) = -F(s)\ \frac{c}{\zeta_o a}\ \frac{e^{-sa/c}}{s}\quad (-1)^n\ \varepsilon_n\left[\frac{s-s_{nm}}{K_n'\left(\frac{sa}{c}\right)}\right]_{s=s_{nm}} \tag{50}$$

s_{nm} is the mth root of $K_n'\left(\frac{sa}{c}\right)$ function.

Similarly, we can show that

$$\vec{E}_{\phi}^{sr}(\phi,s) = \sum_{n=0}^{\infty} \sum_{m=0}^{\infty} C_{nm}(s) \cos n\phi (s-s_{nm})^{-1} \tag{51}$$

where

$$C_{nm}(s) = -F(s) \sqrt{\frac{\pi c}{2sr}} e^{-s(r+a)/c} (-1)^n \varepsilon_n I_n'(\frac{sa}{c}) \left[\frac{s-s_{nm}}{K_n'(\frac{sa}{c})}\right]_{s=s_{nm}} \tag{52}$$

Now, if we desire to obtain a backscattered field $E_{\phi}^{sr}(\phi=\pi,s)$ which contains only a single natural mode (the jlth mode), the required waveform $F_{jl}(s)$ can be determined as

$$F_{jl}(s) = \frac{\left[\frac{1}{s-s_{jl}} + \frac{1}{s-s_{jl}^*}\right] \text{ or } \left[\frac{-j}{s-s_{jl}} + \frac{j}{s-s_{jl}^*}\right]}{\sum_{n=0}^{\infty} \varepsilon_n I_n'(\frac{sa}{c}) \left[\left(\frac{s-s_{nm}}{K_n'(\frac{sa}{c})}\right)_{s=s_{nm}} (s-s_{nm})^{-1} + \left(\frac{s-s_{nm}^*}{K_n'(\frac{sa}{c})}\right)_{s=s_{nm}^*} (s-s_{nm}^*)^{-1}\right]} \tag{53}$$

$F_{jl}(s)$ involves an infinite series of Modified Bessel functions and its inverse Laplace transform is quite complicated. We will seek for an appropriate method to evaluate the real-time function of $F_{jl}(t)$ in the future.

3.2 A Sphere

We have also initiated the study on a perfectly conducting sphere of radius a being illuminated by a radar signal propagating in the + z-direction. The geometry is depicted in fig. 12, and the incident electric field can be expressed as

$$\vec{E}^{inc}(\vec{r},t) = \hat{x}F[t-(z+a)/c]\ U[t-(z+a)/c], \tag{54}$$

and in its Laplace transform as

$$\vec{E}^{inc}(\vec{r},s) = F(s)e^{-\gamma a}[\hat{x}e^{-\gamma R\cos\phi}] \tag{55}$$

where $\gamma = s/c$, and $F(s)$ represents the waveform of the incident radar signal.

After a long derivation, the scattered electric field $\vec{E}^s(\vec{r},s)$ at any point in space can be found, based on the boundary condition on the spherical surface, as

$$\vec{E}^s(\vec{r},s) = -F(s)e^{-\gamma a}\sum_{n=1}^{\infty}(-1)^n\frac{2n+1}{n(n+1)}\Bigg[\left(\frac{i_n(\gamma a)}{k_n(\gamma a)}\right)\vec{M}^{(k)}_{oln} - \left(\frac{\frac{\partial}{\partial R}[Ri_n(\gamma R)]}{\frac{\partial}{\partial R}[Rk_n(\gamma R)]}\right)_{R=a}\vec{N}^{(k)}_{eln}\Bigg] \tag{56}$$

where

$$\vec{M}^{(k)}_{oln} = \frac{1}{\sin\theta}k_n(\gamma R)P^1_n(\cos\theta)\cos\phi\,\hat{\theta} - k_n(\gamma R)\frac{\partial P^1_n(\cos\theta)}{\partial\theta}\sin\phi\,\hat{\phi}$$

$$\vec{N}^{(k)}_{eln} = \frac{n(n+1)}{\gamma R}k_n(\gamma R)P^1_n(\cos\theta)\cos\phi\,\hat{R} + \frac{1}{\gamma R}\frac{\partial}{\partial R}[R\,k_n(\gamma R)]\frac{\partial P^1_n(\cos\theta)}{\partial\theta}\cos\phi\,\hat{\theta} - \frac{1}{\gamma R\sin\theta}\frac{\partial}{\partial R}[R\,k_n(\gamma R)]P^1_n(\cos\theta)\sin\phi\,\hat{\phi}$$

and $i_n(\zeta)$ and $k_n(\zeta)$ are the modified spherical Bessel functions of order n, and $p^1_n(\cos\theta)$ is the associated Legendre function.

The backscattered electric field in the far zone of the sphere can be obtained as

$$\vec{E}^{sr}(s) = [\vec{E}^{s}(\vec{r},s)]_{\substack{R=\infty\\ \theta=\pi\\ \phi=\pi}} = \hat{x}\,\frac{\pi^2}{8}\,F(s)\,\frac{e^{-\gamma(R_\infty+a)}}{R_\infty a}\;\cdot$$

$$\cdot\;\frac{1}{\gamma^2}\sum_{n=1}^{\infty}\frac{2n+1}{k_n(\gamma a)\left[\frac{\partial}{\partial R}(Rk_n(\gamma R))\right]_{R=a}} \tag{57}$$

where R_∞ is the distance between the center of the sphere and the observation point. Equation (19) can be further simplified to

$$\vec{E}^{sr}(s) = -\hat{x}\,\frac{a}{2}\,\frac{e^{-\gamma(R_\infty-a)}}{R_\infty}\;E_1(s) \tag{58}$$

where

$$E_1(s) = \frac{F(s)}{\zeta}\sum_{n=1}^{\infty}\frac{(2n+1)\zeta^{2n+1}}{f_n(\zeta)\,g_n(\zeta)} \tag{59}$$

and

$$\zeta = \gamma a = sa/c.$$

To synthesize F(s) so that the backscattered field contains only a single natural mode (the αth mode), we can equate $E_1(s)$ to $\left(\frac{1}{s-s_\alpha}+\frac{1}{s-s_\alpha^*}\right)$ or $\left(\frac{-j}{s-s_\alpha}+\frac{j}{s-s_\alpha^*}\right)$. With this step we can determine the required waveform $F_\alpha(s)$ as

$$F_\alpha(s) = \left[\frac{\sum_{n=1}^{N} f_n(\zeta)\, g_n(\zeta)}{\sum_{n=1}^{N} (2n+1)\zeta^{2n} \sum_{\substack{m=1 \\ m\neq n}}^{N} f_m(\zeta)\, g_m(\zeta)} \right] \left[\begin{array}{c} \left(\frac{1}{s-s_\alpha} + \frac{1}{s-s_\alpha^*}\right) \\ \text{or} \\ \left(\frac{-j}{s-s_\alpha} + \frac{j}{s-s_\alpha^*}\right) \end{array} \right] \tag{60}$$

where

$$f_n(\zeta) = \sum_{\beta=0}^{n} \frac{(n+\beta)!}{\beta!\,(n-\beta)!} \frac{1}{2^\beta} \zeta^{n-\beta} \tag{61}$$

$$g_n(\zeta) = \sum_{\beta=0}^{n} \frac{(n+\beta)!}{\beta!\,(n-\beta)!} \frac{1}{2^\beta} (\beta+\zeta)\zeta^{n-\beta} \tag{62}$$

s_α is a root of $f_n(\zeta) = 0$ or $g_n(\zeta) = 0$.

N is the maximum number of terms to be considered in the numerical calculation.

At present, efforts are being made to invert $E_1(s)$ for some typical waveforms of F(s) from Equation (59), and to evaluate the real-time function of the required waveform $F_\alpha(t)$ by inverting Equation (60).

3.3 A Wire under Oblique Excitation

We are also considering the case of a thin wire being illuminated by a radar signal at an oblique angle of θ as shown in fig. 13. This case is more general than the case of a thin wire illuminated by a radar signal at normal incidence as discussed in section 2.

We have obtained the required waveform for the incident radar signal to excite a return radar signal which contains only a single natural mode of resonance as follows:

$$F_j(s) = \frac{\left[\frac{1}{s-s_j} + \frac{1}{s-s_j^*}\right] \text{ or } \left[\frac{-j}{s-s_j} + \frac{j}{s-s_j^*}\right]}{\sum_{\alpha=1}^{N} \frac{s^2}{\alpha^2} \left[\frac{1-(-1)^{\alpha} e^{-sL\cos\theta/c}}{1+\left(\frac{sL}{\alpha c\pi}\cos\theta\right)^2}\right]^2 \left[\frac{1}{s_\alpha(s-s_\alpha)} + \frac{1}{s_\alpha^*(s-s_\alpha^*)}\right]} \tag{63}$$

The denominator of $F_j(s)$ contains coefficients which are functions of exponential functions of s. Thus, it is not possible to express $F_j(s)$ as a ratio of two polynomials of s. Therefore, the real-time function of $F_j(t)$ cannot be obtained by our existing Computer Program. Another difficulty encountered was a positive real root for $F_j(s)$ causing $F_j(t)$ to diverge. We plan to overcome these difficulties by seeking a more accurate solution for the induced current on the wire, and developing an appropriate method for inverting $F_j(s)$.

4. Future Plans

We will continue the studies on the infinite cylinder, the sphere and the wire under oblique excitation as described in section 3. Other targets with more complex geometries may also be considered. After these theoretical studies have been completed, we plan to initiate the experimental study to verify the theoretical findings.

5. Personnel

The following personnel has participated in this research program:

1. Kun-Mu Chen, Professor, Principal Investigator
2. Dennis P. Nyquist, Professor, Senior Investigator
3. Che-I Chuang, Graduate Assistant
4. Doug Westmoreland, Graduate Assistant

Appendix A: A Direct Method of Inverting Laplace Transform

A method developed by Liou [13] for evaluating the transient response of a linear system can be applied to determine the real-time waveforms in our study. Since electromagnetists may not be familiar with this method, it is briefly outlined here.

Consider a linear differential equation with constant coefficients

$$x'''(t) + \alpha x''(t) + \beta x'(t) + \gamma x(t) = o \qquad \text{(a1)}$$

with initial values $x(o^+)$, $x'(o^+)$ and $x''(o^+)$.

Taking the Laplace transform of eq. (a1) and rearranging gives

$$X(s) = \frac{x(o^+)s^2 + [x'(o^+) + \alpha x(o^+)]s + [x''(o^+) + \alpha x'(o^+) + \beta x(o^+)]}{s^3 + \alpha s^2 + \beta s + \gamma} \qquad \text{(a2)}$$

This is a ratio of two polynomials in s of the proper form (that is, the degree of the numerator is less than that of the denominator). In general, if

$$X(s) = \frac{a_{m-1}s^{m-1} + a_{m-2}s^{m-2} + \ldots\ldots + a_1 s + a_o}{s^m + b_{m-1}s^{m-1} + \ldots\ldots\ldots\ldots + b_1 s + b_o} \qquad \text{(a3)}$$

where m is a positive integer and a's and b's are arbitrary constants, then the corresponding differential equation is

$$x^m(t) + b_{m-1}x^{(m-1)}(t) + \ldots\ldots + b_1 x'(t) + b_o x(t) = o \qquad \text{(a4)}$$

with initial values

$$x(o^+) = a_{m-1}$$

$$x'(o^+) = a_{m-2} - b_{m-1}x(o^+)$$

$$x''(o^+) = a_{m-3} - b_{m-1}x'(o^+) - b_{m-2}x(o^+)$$

....

$$x^{(m-1)}(o^+) = a_o - b_{m-1}x^{(m-2)}(o^+) - b_{m-2}x^{(m-3)}(o^+) \ldots . - b_1 x(o^+) \tag{a5}$$

The state space equation corresponding to eq. (a4) is

$$x'(t) = A\ x(t) \tag{a6}$$

where

$$x(t) = \begin{bmatrix} x(t) \\ x'(t) \\ \vdots \\ x^{(m-1)}(t) \end{bmatrix} \tag{a7}$$

$$A = \begin{bmatrix} 0 & 1 & 0 & \ldots & 0 & 0 \\ 0 & 0 & 1 & \ldots & 0 & 0 \\ \cdot & & & & & \cdot \\ \cdot & & & & & \cdot \\ \cdot & & & & & \cdot \\ 0 & 0 & 0 & & 0 & 0 \\ -b_o & -b_1 & -b_2 & \ldots & -b_{m-2} & -b_{m-1} \end{bmatrix} \tag{a8}$$

The elements of the initial vector are given by (a5).

Thus, for a given ratio of two polynomials in s of proper form, the corresponding state space equation can be formulated in eq. (a6).

The exact solution of eq. (a6) is

$$x(t) = e^{At}\ x(o^+) \tag{a9}$$

where e^{At} is the transition matrix.

The transition matrix can be expressed by the infinite matrix series

$$e^{At} = \sum_{k=o}^{\infty} \frac{A^k t^k}{k!}, \quad A^o = I = \text{identity matrix} \tag{a10}$$

From eq. (a9) and the properties of the transition matrix, a recursive formula can be derived as

$$x[(n+1)T] = e^{AT}\ x(nT),\ n = 0,1,2,\ldots \tag{a11}$$

where T is an increment of time.

Since the matrix series of eq. (a10) is uniformly convergent in any finite interval, the matrix e^{AT} in eq. (a11) can be evaluated within prescribed accuracy. Once e^{AT} is determined, the vector $x(t)$ at any t can be evaluated based on eq. (a11) with the initial vector $x(o^+)$ as the starting point. The first element of vector $x(t)$ is the desired transient response.

We have developed a computer program based on this method to invert the Laplace transform of the waveform, and another computer program to evaluate the coefficients of a polynomial of s which is originally expressed as a product of many factors of $(s-s_\alpha)$.

Appendix B: An Alternative Solution for the Induced Current

As mentioned in section 2.1, an alternative solution for the amplitude of the natural mode of the induced current can be obtained through a different derivation. This result corresponds to the Class 2 coupling coefficient of Baum [9].

If we assume that

$$I_1(z,s) = \sum_{\alpha=1}^{\infty} a_\alpha(s)\nu_\alpha(z')(s-s_\alpha)^{-1} \tag{B1}$$

with $a_\alpha(s)$ as a function s, and through a somewhat different derivation than that given in section 2.1, we will have

$$a_\alpha(s) = \frac{\int_o^L dz\ \nu_\alpha(z)\ V(s)}{\int_o^L dz\ \nu_\alpha(z)\left[\int_o^L \Gamma_{1\alpha}(z,z')\nu_\alpha(z')dz'\right]} \tag{B2}$$

This can be evaluated to be

$$a_\alpha(s) = K\left(\frac{1}{\alpha}\right)\left(\frac{s}{s_\alpha}\right) \quad \text{for } \alpha=\text{odd} \tag{B3}$$

$$= 0 \quad \text{for } \alpha=\text{even}$$

With this $a_\alpha(s)$, the induced current on the wire due to the excitation of $\vec{E}^{inc}(z,s) = \hat{z}\, F(s)$ can be obtained as

$$I(z,s) = K \sum_{\alpha=odd}^{N} F(s)\frac{1}{\alpha} \sin\left(\frac{\alpha\pi z}{L}\right)\left[\frac{s}{s_\alpha(s-s_\alpha)} + \frac{s}{s_\alpha^*(s-s_\alpha^*)}\right]$$

$$= K \sum_{\alpha=odd}^{N} F(s)\frac{1}{\alpha} \sin\left(\frac{\alpha\pi z}{L}\right)\left[\frac{1}{s-s_\alpha} + \frac{1}{s-s_\alpha^*} + \frac{1}{s_\alpha} + \frac{1}{s_\alpha^*}\right] \quad (B4)$$

It is noted that this solution differs from I(z,s) given in eq. (22) by a small negative term of

$$K \sum_{\alpha=odd}^{N} F(s)\frac{1}{\alpha} \sin\left(\frac{\alpha\pi z}{L}\right)\left(\frac{1}{s_\alpha} + \frac{1}{s_\alpha^*}\right) = K \sum_{\alpha=odd}^{N} F(s)\frac{1}{\alpha} \sin\left(\frac{\alpha\pi z}{L}\right)\left(\frac{-2\sigma_\alpha}{|s_\alpha|^2}\right) \quad (B5)$$

The backscattered electric field maintained by I(z,s) can be determined as

$$E^s(s) = K_1 \frac{e^{-sR_\infty/c}}{R_\infty} \sum_{\alpha=odd}^{N} s\, F(s)\frac{1}{\alpha^2}\left[\frac{1}{s-s_\alpha} + \frac{1}{s-s_\alpha^*} + \frac{1}{s_\alpha} + \frac{1}{s_\alpha^*}\right] \quad (B6)$$

Based on the expression of I(z,s) given in eq. (B4), an equivalent circuit for the target can be constructed. It is a network of N parallel circuits with each circuit synthesized with a capacitor, an inductor, a series resistor, and a negative resistance connected across the inductor. This negative resistance is due to the presence of the negative term of eq. (B5) in the induced current I(z,s) of eq. (B4). This negative term leads to a non-physical situation even though it gives a better asymptotic behavior of I(z,s) for the step excitation, F(s) = 1/s. The phenomenon of negative resistance was also observed by other worker [14]. On the other hand, the backscattered electric field $E^s(s)$ given in eq. (B6) gives the following results: for the impulse excitation, F(s) = 1, $E^s(s)$ exhibits a derivative of a delta function at t=o; for the step excitation, F(s) = 1/s, $E^s(s)$ exhibits a delta function at t=o; and for the ramp excitation, $F(s) = 1/s^2$, $E^s(s)$

contains a constant component and a finite value at t=o. These results on the backscattered electric field deviate from experimental observations.

This alternative solution of I(z,s) has more discrepancies than the solution of I(z,s) given in eq. (22), even though the latter is also approximate in nature. For these reasons, this alternative solution of the induced current is not used in this study.

It is also noted that with $E^S(s)$ as given in eq. (B6), it is not possible to synthesize a waveform F(s) for producing a pure natural mode of $E^S(s)$ because the negative term, $(1/s_\alpha+1/s_\alpha{}^*)$, in eq. (B6) will cause F(s) to diverge. However, if the incident radar signal with $F_1(s)$ given in eq. (37) is used in eq. (B6), the backscattered field $E_1^S(s)$ calculated from eq. (B6) will exhibit the first natural mode of resonance (with a zero initial value) modified by a small near-constant term. This example tends to indicate that the required waveforms F(s) synthesized in section 2.3 for exciting single natural mode, return radar signals may remain rather invariant even if a more accurate induced current is used.

References

(1) E. K. Kennaugh and D. L. Moffatt, "Transient and impulse response approximation," Proc. of IEEE, Vol. 53, pp. 893-901, August 1965.

(2) D. L. Moffatt and R. K. Mains, "Detection and discrimination of radar targets," IEEE Trans. on Ant. and Prop., Vol. AP-23, No. 3, pp. 358-367, May 1975.

(3) A. J. Berni, "Target identification by natural resonance estimation," IEEE Trans. on Aerospace and Electronic Systems, Vol. AES-11, No. 2, pp. 147-154, March 1975.

(4) J. D. Young, "Radar imaging from ramp response signatures," IEEE Trans. on Ant. and Prop., Vol. AP-24, No. 3, pp. 276-282, May 1976.

(5) K. A. Shubert, J. D. Young and D. L. Moffatt, "Synthetic radar imagery," IEEE Trans. on Ant. and Prop., Vol. AP-25, No. 4, pp. 477-483, July 1977.

(6) C. L. Bennett, W. Weeks, "A technique for computing approximate electromagnetic impulse response of conducting bodies," Purdue University, Lafayette, Indiana, Tech. Report TR-EE68-11, 1968.

(7) A. G. Repjar, A. A. Ksienski and L. J. White, "Object identification from multi-frequency radar returns," The Radio and Electronics Engineers, Vol. 45, No. 4, pp. 161-167, April 1975.

(8) C. W. Chuang and D. L. Moffatt, "Natural resonance of radar target via Prony's method and target discrimination," IEEE Trans. on Aerospace and Electronic Systems, Vol. AES-12, No. 5, pp. 583-589.

(9) C. E. Baum, "The singularity expansion method," Transient Electromagnetic Fields, Editor: L. B. Felsen, pp. 130-176, 1976.

(10) F. M. Tesche, "On the analysis of scattering and antenna problems using the singularity expansion techniques," IEEE Trans. on Ant. and Prop., Vol. AP-21, No. 1, pp. 53-62, January 1973.

(11) L. Marin, "Natural-mode representation of transient scattering from rotationally symmetric bodies," IEEE Trans. on Ant. and Prop., Vol. AP-22, No. 2, pp. 266-274, March 1974.

(12) M. L. Van Blaricum and R. Mittra, "A technique for extracting the poles and residues of a system directly from its transient response," IEEE Trans. on Ant. and Prop., Vol. AP-23, No. 6, pp. 777-781, November 1975.

(13) M. L. Liou, "A novel method of evaluating transient response," Proc. of IEEE, Vol. 54, No. 1, pp. 20-23, January 1966.

(14) D. R. Wilton and L. W. Pearson, "Analytic properties of some SEM-Derived quantities," presented in 1979 Fall URSI Meeting, Univ. of Colorado, Nov. 1979.

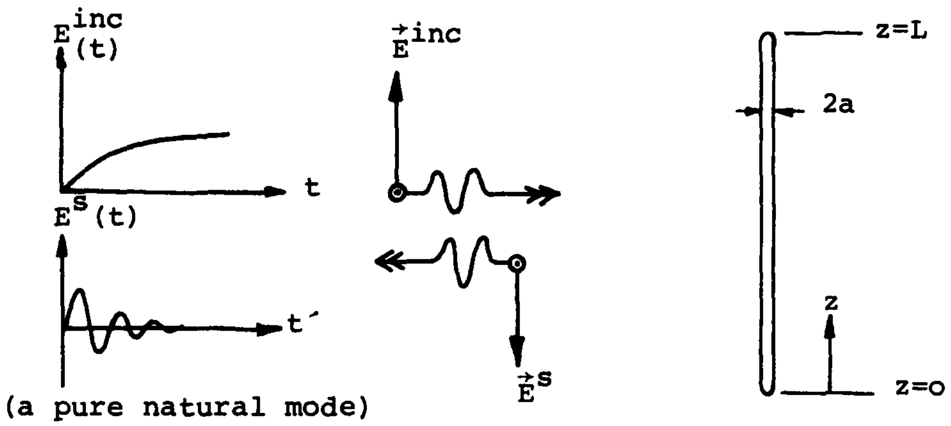

fig. 1. A thin wire illuminated by a radar signal at normal incidence.

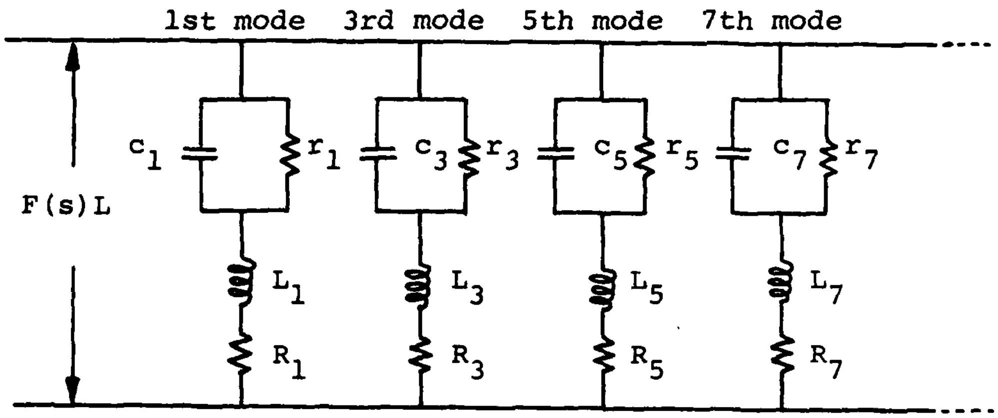

$$L_\alpha = \left(\frac{L}{K}\right)\frac{\alpha}{2} \quad , \quad c_\alpha = \left(\frac{K}{L}\right)\frac{2}{\alpha}\,\frac{1}{\omega_\alpha^2}$$

$$R_\alpha = \left(\frac{L}{K}\right)\frac{\alpha}{2}\,\sigma_\alpha \quad , \quad r_\alpha = \left(\frac{L}{K}\right)\frac{\alpha}{2}\,\frac{\omega_\alpha^2}{\sigma_\alpha}$$

where $s_\alpha = -\sigma_\alpha + j\omega_\alpha$

$$\frac{L}{K} = [2 \log \left(\frac{L}{a}\right) - 1]\,\mu_o L/8 \quad \text{(henry)}$$

fig. 2. An equivalent circuit for the wire target.

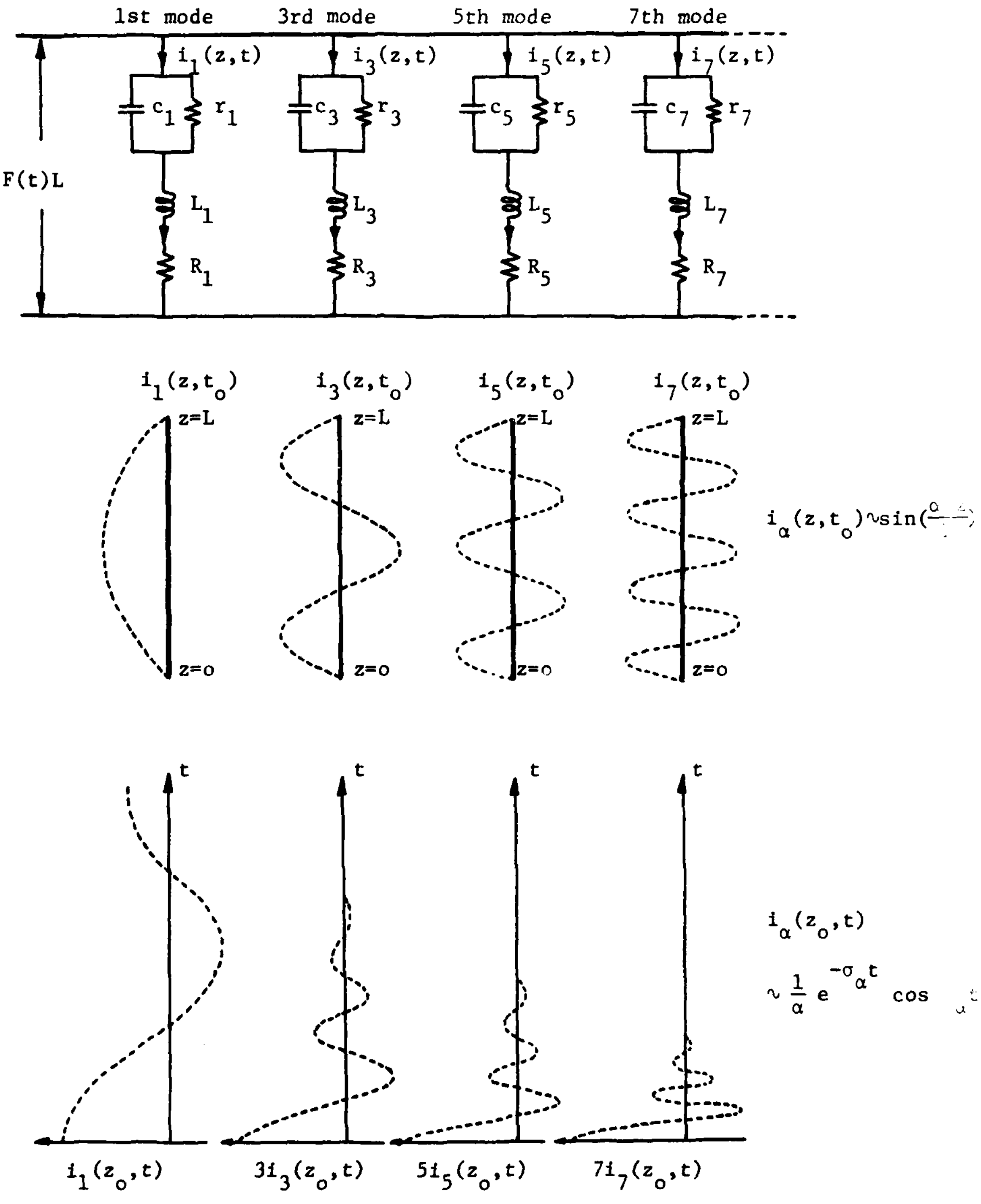

fig. 3. Spatial and temporal variations of various natural modes of currents induced by an impulse excitation in the equivalent circuit of the target.

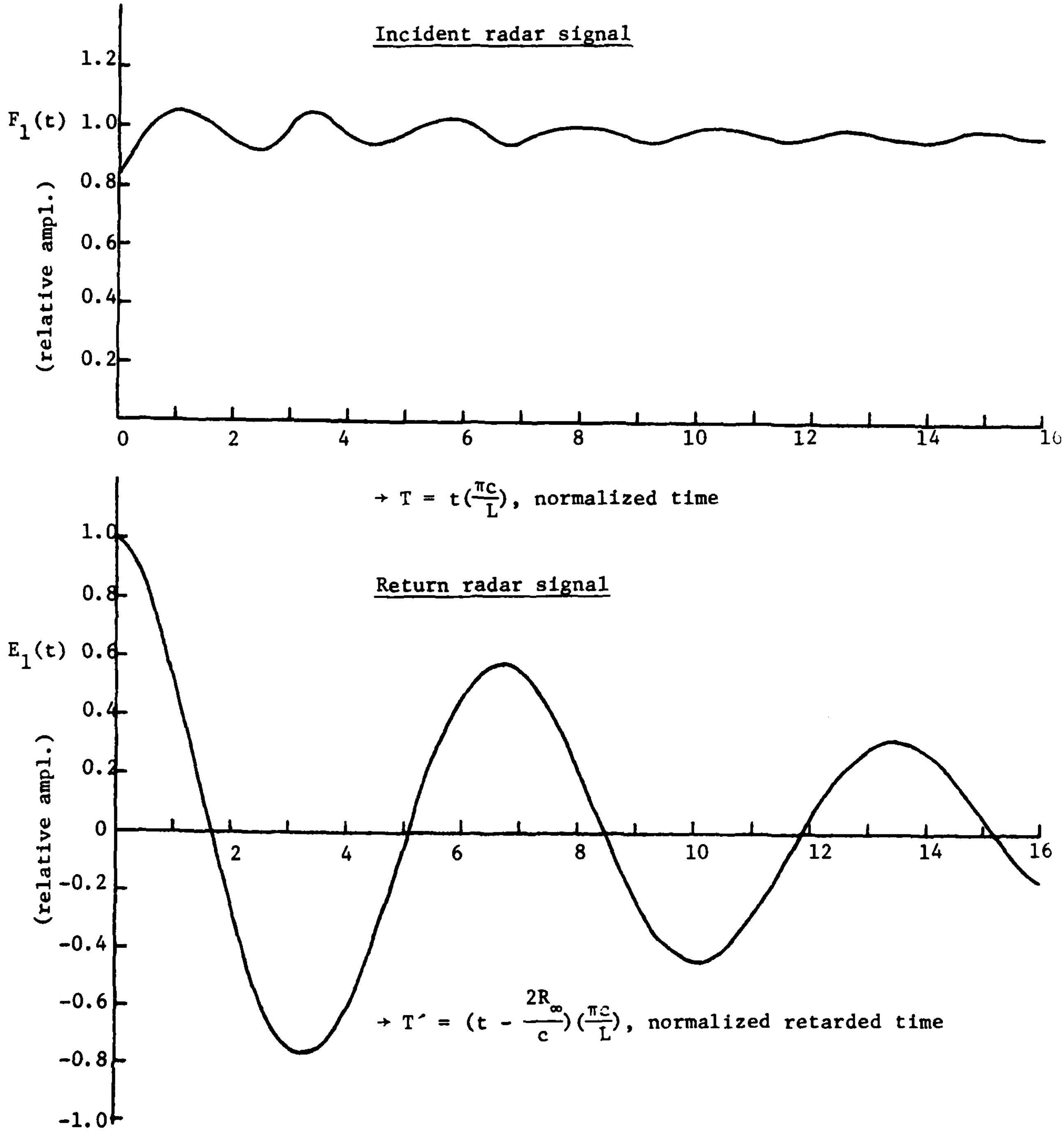

fig. 4. Waveforms of the incident and return radar signals; the former is synthesized to excite a thin wire to produce the latter which contains only the first natural resonance mode (with a maximum initial value) of the wire.

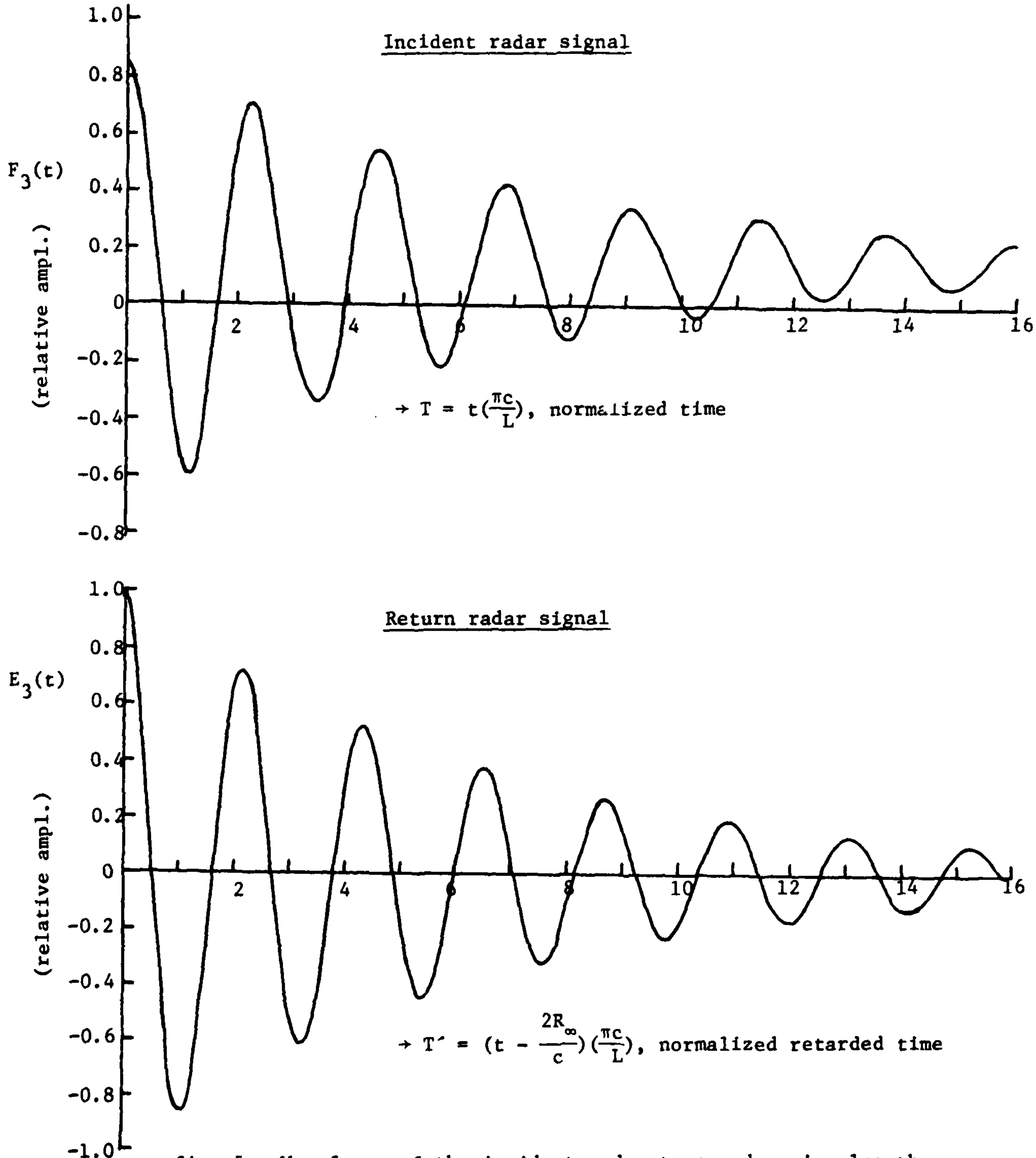

fig. 5. Waveforms of the incident and return radar signals; the former is synthesized to excite a thin wire to produce the latter which contains only the third natural resonance mode (with a maximum initial value) of the wire.

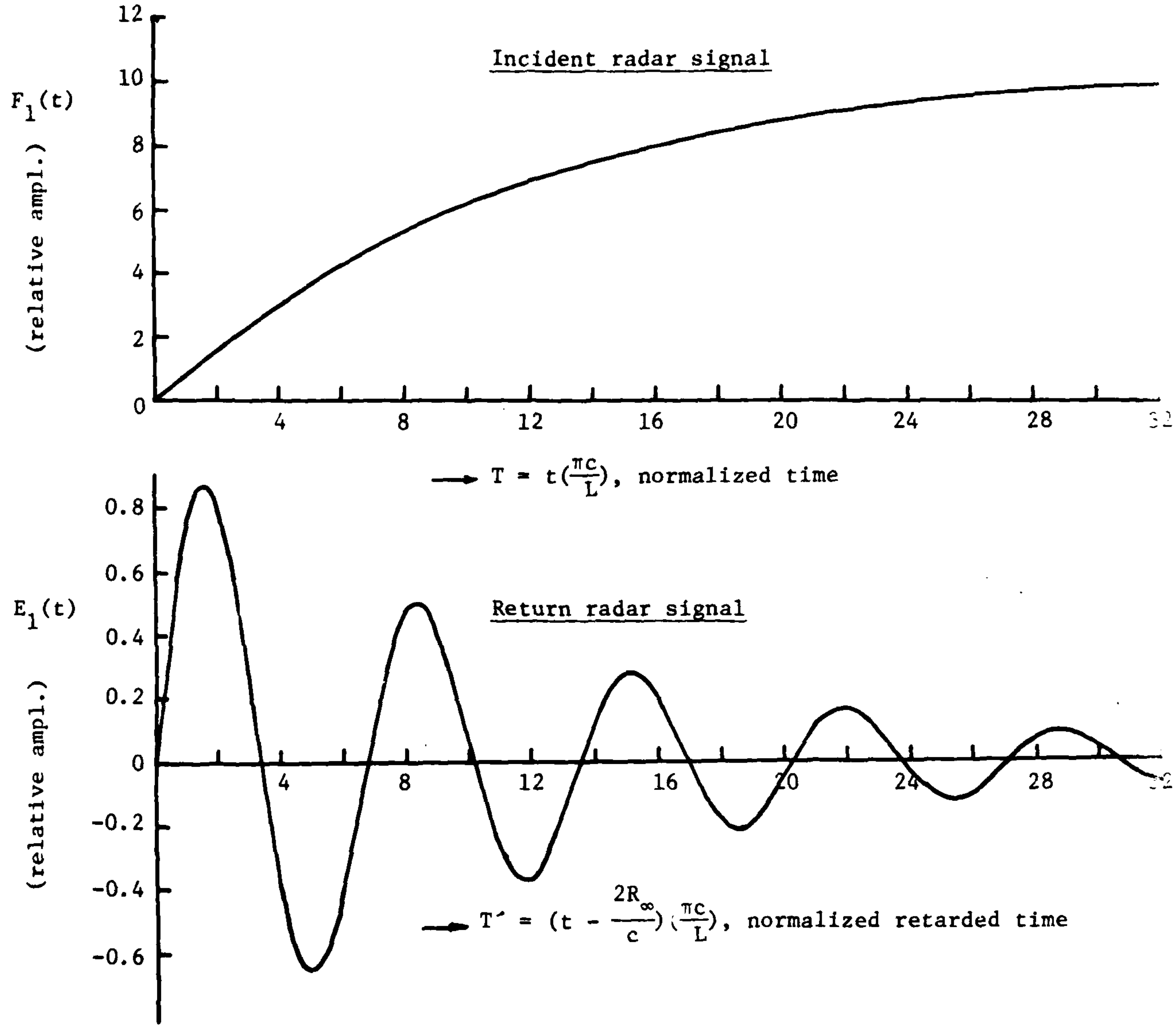

fig. 6. Waveforms of the incident and return radar signals; the former is synthesized to excite a thin wire to produce the latter which contains only the first natural resonance mode (with a zero initial value) of the wire.

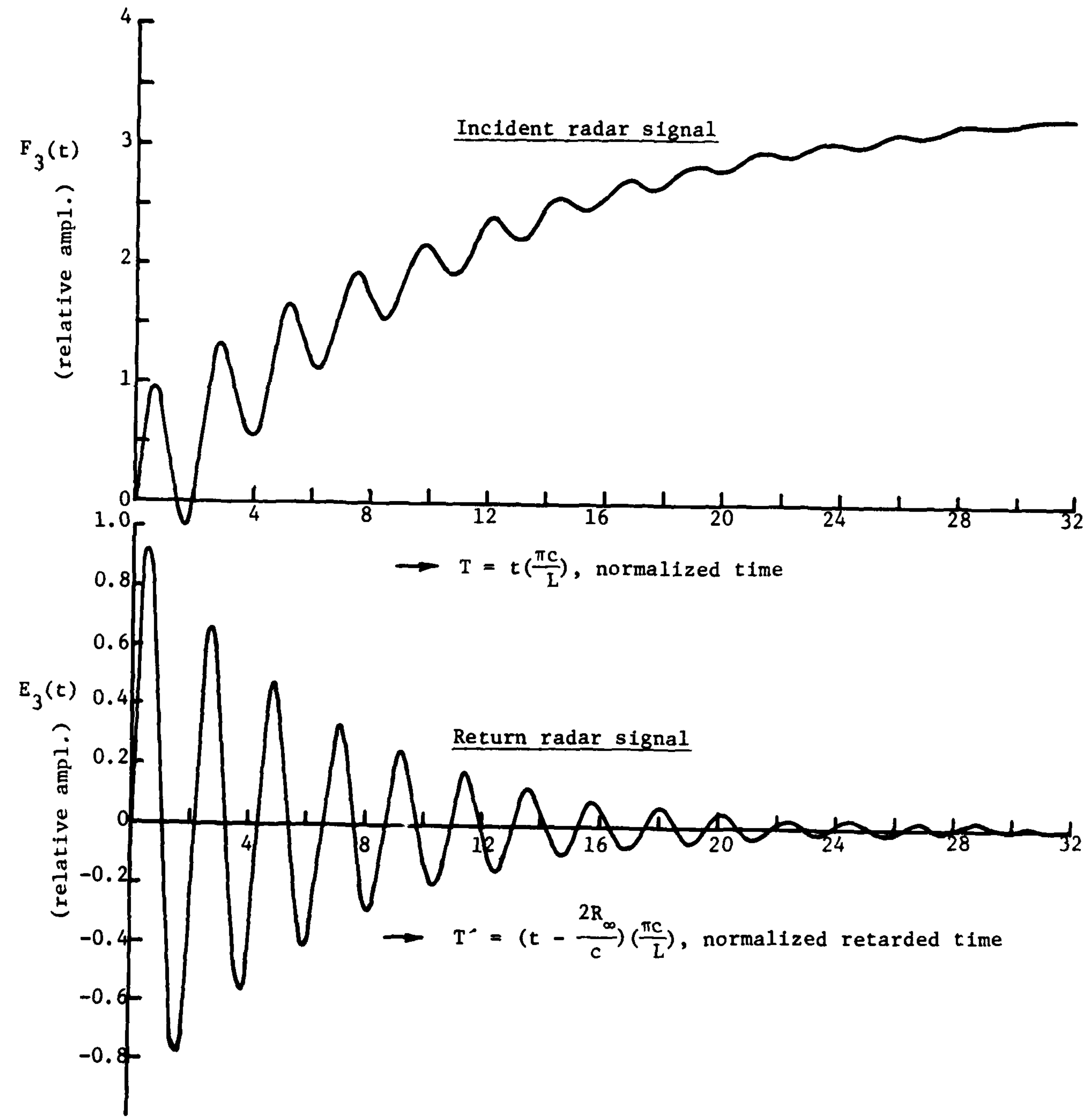

fig. 7. Waveforms of the incident and return radar signals; the former is synthesized to excite a thin wire to produce the latter which contains only the third natural resonance mode (with a zero initial value) of the wire.

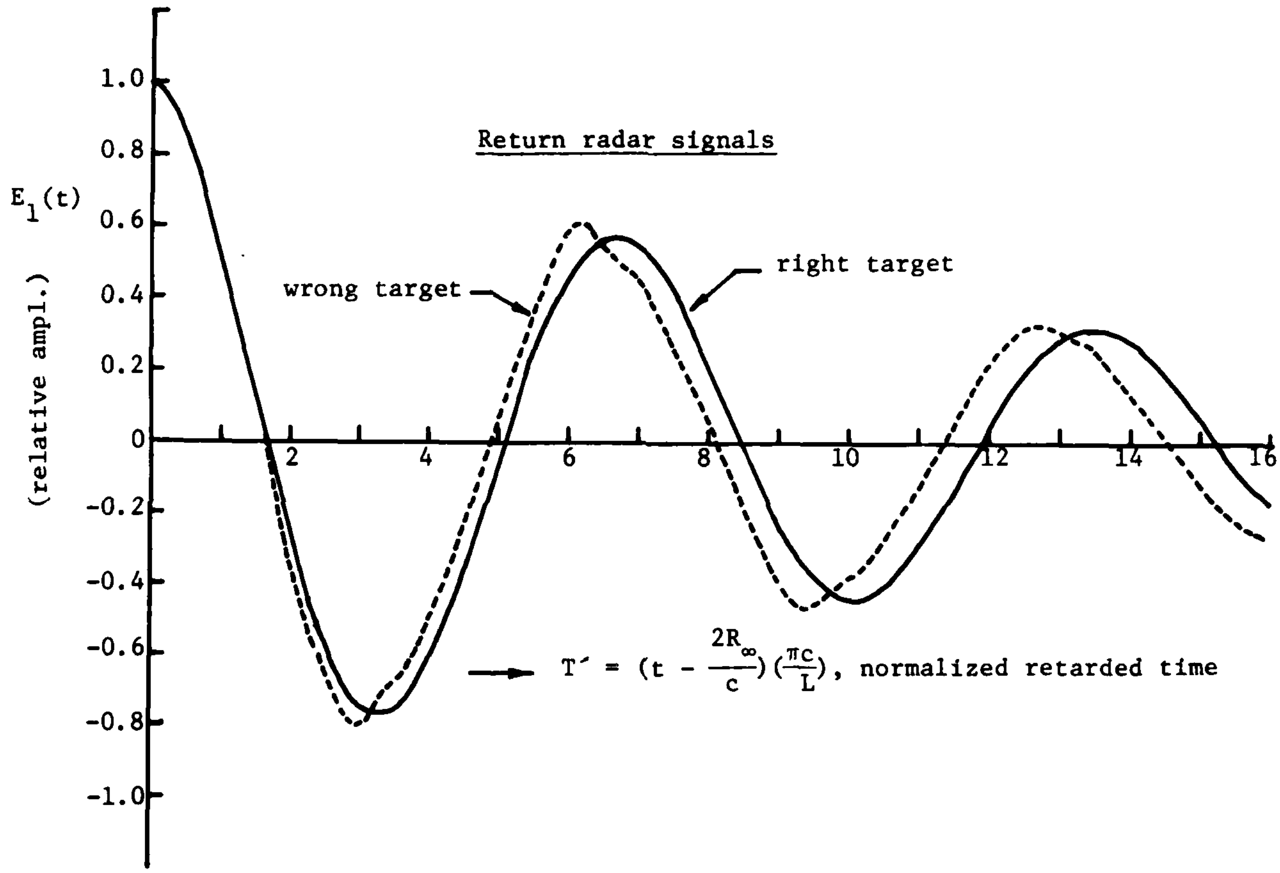

fig. 8. Waveforms of return radar signals from the right target and a wrong target when the incident radar signal is synthesized to excite the first natural resonance mode (with a maximum initial value) of the right target. The wrong target is a thin wire about 5% shorter than the right target which is also a thin wire.

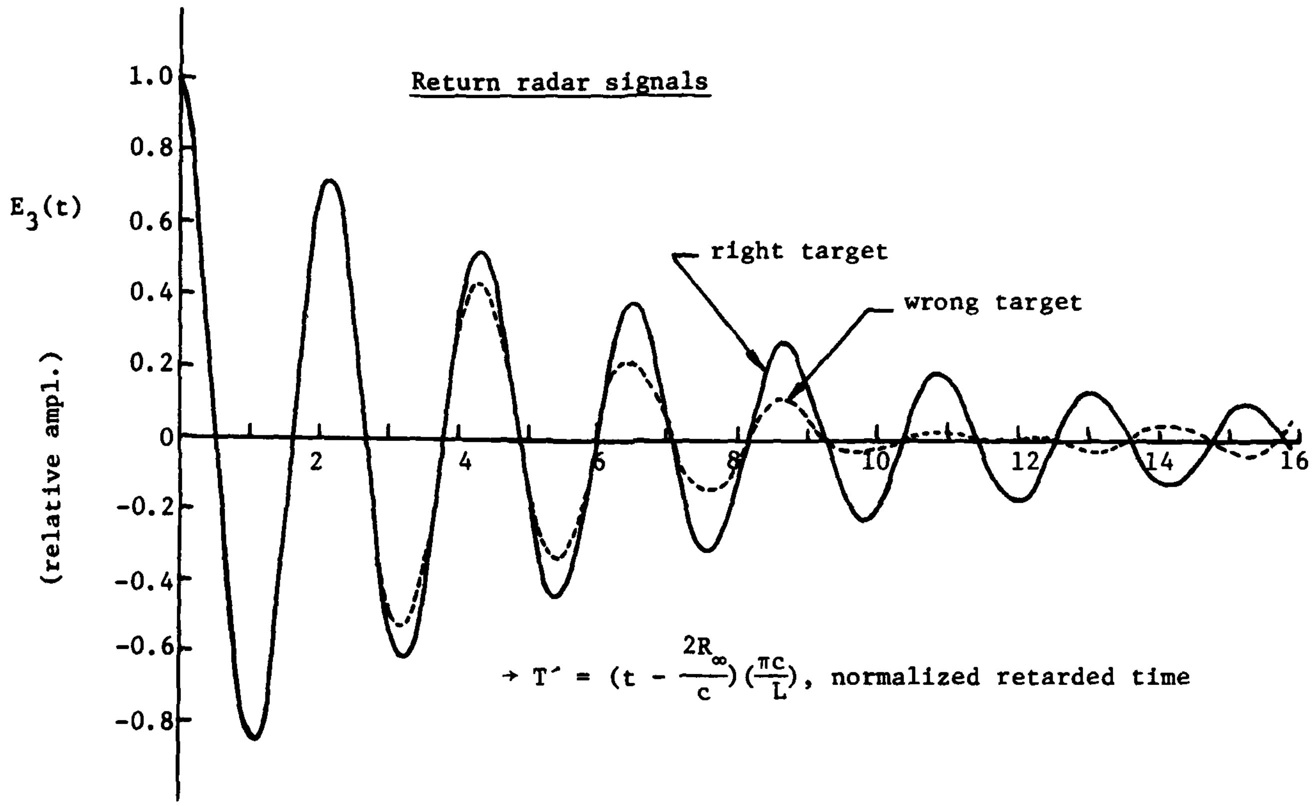

fig. 9. Waveforms of return radar signals from the right target and a wrong target when the incident radar signal is synthesized to excite the third natural resonance mode (with a maximum initial value) of the right target. The right target is a thin wire and the wrong target is also a thin wire but about 5% shorter.

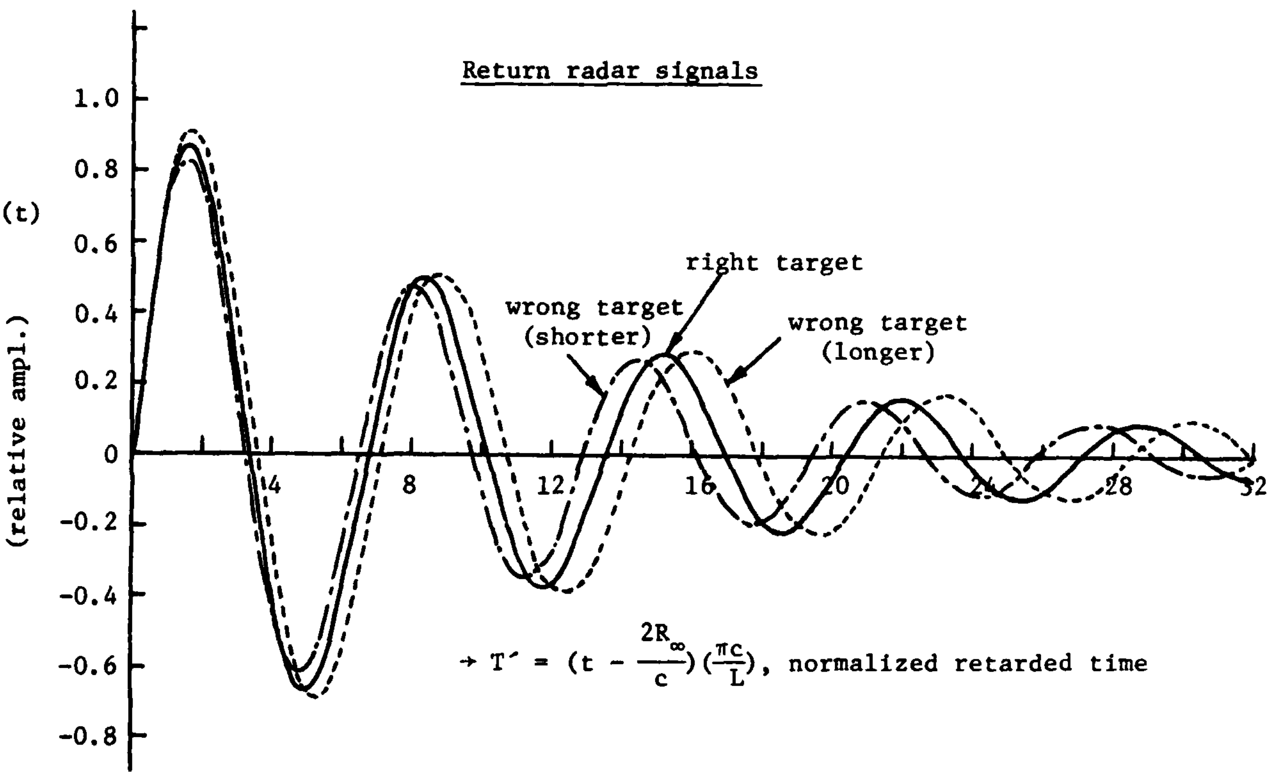

fig. 10. Waveforms of return radar signals from the right target and two wrong targets when the incident radar signal is synthesized to excite the first natural resonance mode (with a zero initial value) of the right target. The right target is a thin wire and the wrong targets are also thin wires, one is 5% shorter and the other 5% longer than the right target.

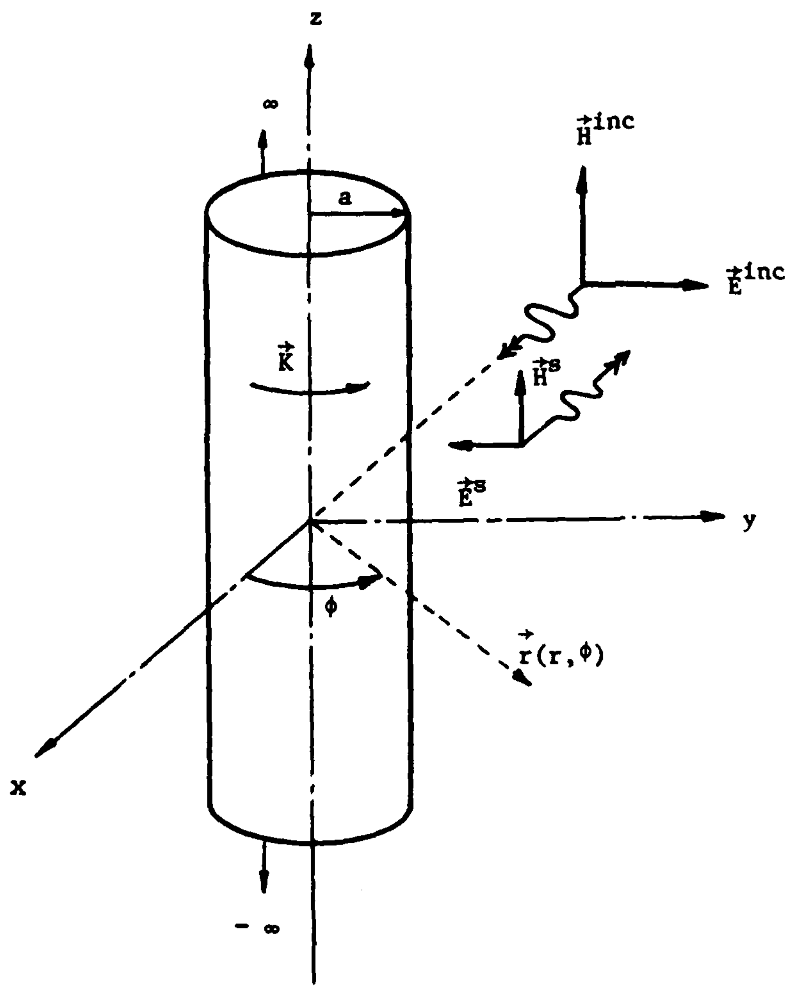

fig. 11. A perfectly conducting, infinite cylinder is illuminated by a radar signal with TM polarization.

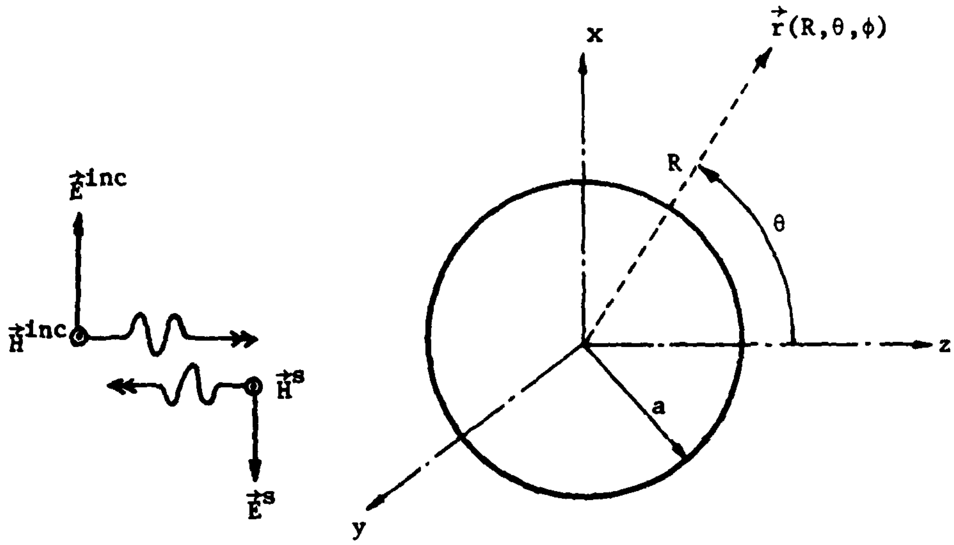

fig. 12. A perfectly conducting sphere of radius a is illuminated by a radar signal propagating in the + z-direction.

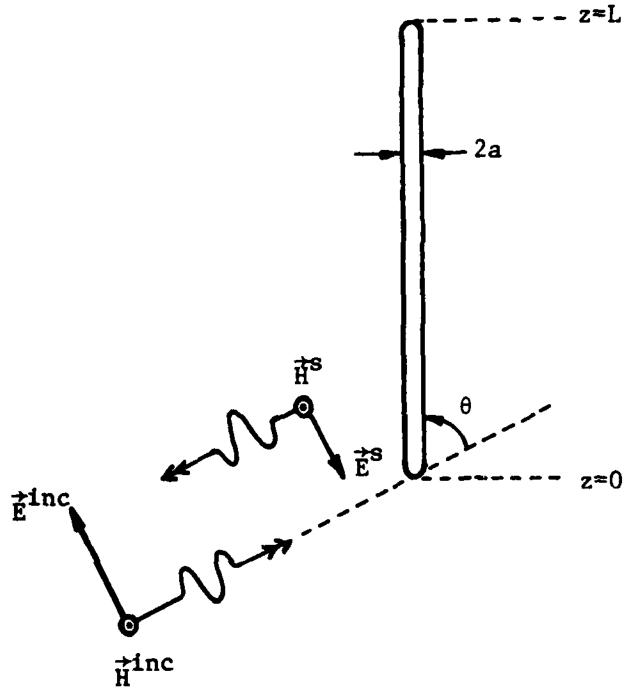

fig. 13. A thin wire is illuminated by a radar signal at an oblique angle.